THE REAL BEHAVIOUR OF COHESIONLESS GRANULAR MATERIALS UNDERGOING DEFORMATION. THE DISTRIBUTION OF THE DEFORMATION IN A FLOWING GRANULAR MATERIAL IN AN EQUIPMENT SATISFYING PRANDTL'S BOUNDARY CONDITIONS*

V.ŠMÍD and J.NOVOSAD

Institute of Chemical Process Fundamentals,
Czechoslovak Academy of Sciences, 165 02 Prague 6 - Suchdol

Received April 16th, 1975

The paper presents an experimental velocity field in a granular solid measured under controlled plastic deformation in an equipment satisfying the boundary conditions of Prandtl's solution. The established velocity field is compared with a theoretical solution obtained from the model due to de Josselin de Jong. The deviations are pointed out from the theoretical solution caused by the real behaviour of the granular material.

This part of study of the real behaviour of granular materials deals with the relation between the real velocity field and a theoretical solution. The paper is a continuation of the preceding parts of this series[1] where a theoretical solution of the field of stress and deformation has been developed for an apparatus satisfying Prandtl's boundary conditions using the model due to de Josselin de Jong. This solution[1] has the following form

$$0 \geqq \frac{2\,\partial v_r}{\partial r} \geqq \left(\frac{\partial v_\Theta}{\partial r} + \frac{1}{r}\frac{\partial v_r}{\partial \Theta} - \frac{v_\Theta}{r}\right) \operatorname{tg} 2\phi \,, \qquad (1)$$

$$\frac{\partial v_r}{\partial r} + \frac{1}{r}\frac{\partial v_\Theta}{\partial \Theta} + \frac{v_r}{r} = 0 \,. \qquad (2)$$

The model of de Josselin de Jong[2] has been chosen because it is a relatively recent model and apparently the most realistic one for expressing the relation between stress and strain. Moreover, in its technical application to two-dimensional cases it suffices that the envelope of the Mohr's circles be known which can be obtained from relatively simple tests.

---

* Part X in the series Studies on Granular Materials; Part IX: This Journal *41*, 1750 (1976).

The experimental field of stress was compared with the theoretical one in the preceding part of this series[3]. Together, these papers represent a full picture of the behaviour of cohesionless granular material in an advanced stage of deformation.

Experimental Values and Description of the Velocity Field

The field of deformations was recorded photographically during the experiments simultaneously with the stress measurements described in the preceding parts. The recording of the velocity field is shown schematically in Fig. 1. Mounting the camera to one of the moving slabs of the wedge facilitates evaluation because the image of the slab (immobile on the picture) served as a frame of reference of the coordinate system 0, r, Θ. Longer exposures were used in order to obtain the streamline pattern. Always five pictures were shot during each deformation cycle between the angles 76°30′ and 50°. These pictures were shot at the angle α equal to 76°30′; 70°; 63°30′; 56°45′ and 51°. The photographs were shot in each experiment and the set taken for evaluation was that whose course of stress approached most closely to the representative average of all experiments.

Fig. 2* is a photograph of streamlines taken as the fifth exposure of the given experiment at an angle $\alpha = 51°$, *i.e.* at an advanced stage of deformation and at a relative constrainment of 35% from the initial value of the angle. The bottom part of the photograph shows steel balls substituting the granular material in the apex of the wedge put there to stop draining of the granular material through the interstices between the rotating parts of the equipment.

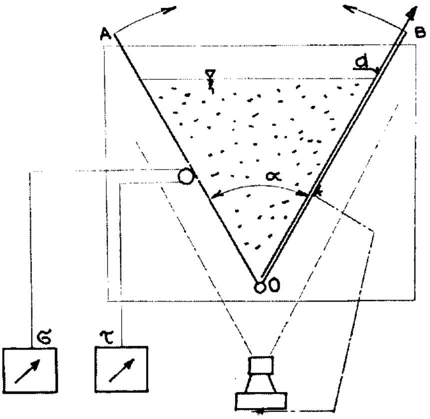

FIG. 1

Experimental Method of Determining Velocity Field

---

* See insert on the opposite p.

From a mathematical point of view the streamlines represent a family of plane curves as

$$r = r(\Theta, C)\,, \tag{3}$$

whose tangent at any point gives the direction of the velocity vector[4] at that point. This is shown schematically in Fig. 3. Thus we may write

$$\frac{\mathrm{d}r}{r\mathrm{d}\Theta} = \frac{v_r(r, \Theta)}{v_\Theta(r, \Theta)} \doteq \mu(r, \Theta)\,. \tag{4}$$

Assuming in accordance with the model of de Josselin de Jong the granular material to be incompressible, the condition of incompressibility, Eq. (2), can be solved with the aid of Eq. (4) for the known boundary conditions apparent from Fig. 3. Eq. (2) arranged with the aid of Eq. (4) takes the form

$$\frac{\mu}{\dfrac{\partial \mu}{\partial r} + \dfrac{\mu}{r}} \frac{\partial v_\Theta}{\partial r} + \frac{1}{\dfrac{\partial}{\partial r}(r\mu)} \frac{\partial v_\Theta}{\partial \Theta} = -v_\Theta\,. \tag{5}$$

A solution of Eq. (5) together with Eq. (4) then represents a description of the velocity field.

For the purpose of a numerical solution of the equations describing the velocity the examined region was divided into three zones as shown schematically in Fig. 4.

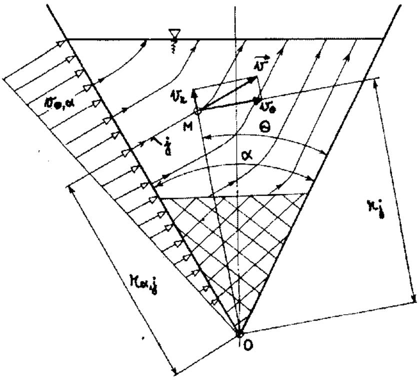

FIG. 3

Velocity Field in Deformed Granular Material

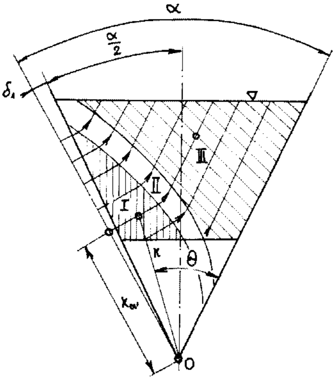

FIG. 4

Velocity Fields in Various Zones

The shape of the streamlines was best represented by two different families of parallel straight lines I and III and by curves in the intermediate region. Theoretical velocity field consisted then of two parts with the following equations valid for zone I

$$v_{rI} = 2{\cdot}693 \,.\, 10^{-3} r \sin(\alpha' - \Theta) \cos(\alpha' - \Theta)\,, \quad [\mathrm{m/s}]$$

$$v_{\Theta I} = 2{\cdot}693 \,.\, 10^{-3} r \cos^2(\alpha' - \Theta)\,, \quad [\mathrm{m/s}]$$

and for zone III

$$v_{rIII} = 7{\cdot}63 \,.\, 10^{-2}[1 - 0{\cdot}1/(0{\cdot}01 + 0{\cdot}0692 r \sin\Theta)^{1/2}] \cos\Theta\,, \quad [\mathrm{m/s}]$$

$$v_{\Theta III} = -7{\cdot}63 \,.\, 10^{-2}[1 - 0{\cdot}1/(0{\cdot}01 + 0{\cdot}0692 r \sin\Theta)^{1/2}] \sin\Theta\,. \quad [\mathrm{m/s}]$$

The magnitude of the radius r is expressed in metres.

By substitution it can be proven that the above expressions satisfy condition (*4*) concerning mutual ratio of the two velocity components because

$$\mu_I = -\mathrm{tg}(\alpha' - \Theta) \quad \text{and} \quad \mu_{III} = -\mathrm{ctg}\,\Theta$$

as well as the assumed incompressibility, Eq. (*2*), in the two regions.

Owing to the small extent of zone II and complicated shape of the streamlines the solution was not sought in this zone.

Comparison of the Velocity Field with the Theoretical Solution

The experimentally determined field of velocities was compared with the theoretical solution according to the model of de Josselin de Jong based on Prandtl's solution by substituting the experimental results into Eqs (*1*) and (*2*). Since, however, the condition of incompressibility, Eq. (*2*), has been already used to determine the real velocity field it has been assumed in fact that the material during advancing deformation undergoes no volume changes. In any case the used experimental technique did not provide for a sufficiently accurate measurement of the volume changes and the incompressibility thus could not be verified.

From a comparison of the condition of deviation of the principal directions of the stress and deformation, Eq. (*1*), it has followed, after substitution and some arrangement, that the behaviour of the material in region III (Fig. 4) and within $0 \leqq \Theta \leqq \phi$ obeys the theoretical solution and that the whole range of the deviation angle $-\phi/2 \leqq \xi \leqq +\phi/2$ becomes effective. In region I, however, the true velocity field did not follow the theoretically predicted distribution.

DISCUSSION

Deformation of the granular material in an equipment satisfying the boundary conditions of Prandtl's solution gave rise to two markedly different regions in the velocity field. The larger zone (III in Fig. 4) satisfies virtually in the whole region the theoretical solution based on the model of de Josselin de Jong, while the smaller one (I) did not obey the theoretically expected solution. The cause of the different behaviour in the two regions rests probably in the necessity for a considerable degree of deformation to reach the limiting state which has been described in Part IX of this series. While in the vicinity of the arm OB of the wedge (Fig. 1) the imposed motion of the slab caused the limiting state to be reached rather quickly along the whole slab, the pressure cell built into the slab OA 330 mm from the apex of the wedge did not detect the limiting state until the wedge has been closed by 19·52% of the original value of the angle OAB. It was this necessity of a considerable degree of deformation that lead to the concept of a gradual mobilization of the limiting state of stress in the direction away from the top surface toward the apex, *i.e.* from position that travelled a longer deformation path. The disagreement between the theoretical and the real behaviour in zone I may thus be explained probably by the need for considerable deformation to reach the limiting state on the existence of which the theoretical solution was based. In our case the deformation path in the vicinity of the apex on the slab OA need not have been sufficiently long to bring all granular material along its length into the state of plastic stress which may have decisively affected the behaviour of the material adhering to this slab.

The real behaviour of the granular material under controlled deformation thus agreed with the theoretical behaviour only in those regions which evidently satisfied the prerequisites of the theoretical solution namely the existence of the limiting state of stress. This assumption though need not be always met by real materials because if plastic deformation causes the initial state of stress to change into a different limiting state this change calls for considerable deformation. At the same time certain areas may exist within the material where the deformation path is not sufficiently long to fully mobilize the expected limiting state and the deformation of the material is then at variance with the theoretical solution based on the limiting state of stress.

LIST OF SYMBOLS

C	constant
r, Θ	polar coordinates
v_r, v_Θ	radial and tangential component of velocity
α	angle of Prandtl's wedge
α'	angle of the normal to the family of streamlines
μ	ratio of radial and tangential component of velocity
ϕ	angle of internal friction of the material
ξ	deviation angle

REFERENCES

1. Šmíd V., Novosad J.: This Journal *41*, 1740 (1976).
2. de Josselin de Jong G.: Géotechnique *21*, 155 (1971).
3. Šmíd V., Novosad J.: This Journal *41*, 1749 (1976).
4. Prandtl L., Titjens O. G.: *Fundamentals of Hydro- and Aeromechanics.* Dover Publications, New York 1957.

Translated by V. Staněk.